Ambient Dataloops: Generative Models for Dataset Refinement

Adrian Rodriguez-Munoz
CSAIL
MIT
adrianrm@mit.edu

William Daspit
Computer Science
UT Austin, IFML
willdaspit@gmail.com

Adam Klivans
Computer Science
UT Austin, IFML
klivans@utexas.edu

Costis Daskalakis
CSAIL
MIT
costis@mit.edu

Antonio Torralba
CSAIL
MIT
torralba@mit.edu

Giannis Daras
CSAIL
MIT
gdaras@mit.edu

Abstract

We propose Ambient Dataloops, an iterative framework for refining datasets that makes it easier for diffusion models to learn the underlying data distribution. Modern datasets contain samples of highly varying quality, and training directly on such heterogeneous data often yields suboptimal models. We propose a dataset-model co-evolution process; at each iteration of our method, the dataset becomes progressively higher quality, and the model improves accordingly. To avoid destructive self-consuming loops, at each generation, we treat the synthetically improved samples as noisy, but at a slightly lower noisy level than the previous iteration, and we use Ambient Diffusion techniques for learning under corruption. Empirically, Ambient Dataloops achieve state-of-the-art performance in unconditional and text-conditional image generation and de novo protein design. We further provide a theoretical justification for the proposed framework that captures the benefits of the data looping procedure.

1 Introduction

Much of the recent progress in generative modeling is attributed to the existence of large-scale, high-quality datasets. Indeed, modern generative models have an appetite for data that is becoming increasingly hard to fulfill (Goyal et al., 2024; Kaplan et al., 2020; Saharia et al., 2022; Hoffmann et al., 2022; Henighan et al., 2020). That triggers the formation of datasets that include any points that are available for training, including synthetic and out-of-distribution data, and naturally, these datasets contain samples of various qualities. The lower-quality parts of the training data are often removed through various filtering techniques (Gadre et al., 2023; Li et al., 2024), either from the beginning of the training or in some intermediate training stage (Sehwag et al., 2025). This approach is optimal when the bottleneck is the computational budget for training, since it is better to allocate the limited compute to the higher-quality training points (Goyal et al., 2024; Hoffmann et al., 2022). However, when the issue is not computational budget, but availability of data, filtering increases quality, but comes at the cost of reduced diversity in the generated outputs (Somepalli et al., 2023a,b; Daras et al., 2024; Prabhudesai et al., 2025; Carlini et al., 2023).

Post-training, diffusion generative models often undergo refinements of all sorts to sample faster (Salimans & Ho, 2022; Song et al., 2023), become aligned with reward models (Domingo-Enrich et al., 2024; Black et al., 2023), or reduce their parameter count (Meng et al., 2023). The noisy dataset that was used to train the model remains, on the contrary, static. We hence ask: *Is it possible to use a model trained on a noisy set to improve the set that it was trained on?*

37th Conference on Neural Information Processing Systems (NeurIPS 2023).

Figure 1: **Dataset and model evolution across loops of our method.** D_0 shows synthetically generated images from DiffusionDB (Wang et al., 2022), a dataset used for text-to-image generative modeling. These images have artifacts due to learning errors of the underlying model. We train a model on this dataset, M_1, that we use to improve its own training set, leading to a "restored" dataset D_1. Successive iterations of this process lead to a co-evolution of both the model and the dataset – see dataset D_2 and model M_1 respectively. We avoid catastrophic self-consuming loops by accounting for learning errors at each iteration using Ambient Diffusion (Daras et al., 2025c, 2023) techniques for learning from imperfect data.

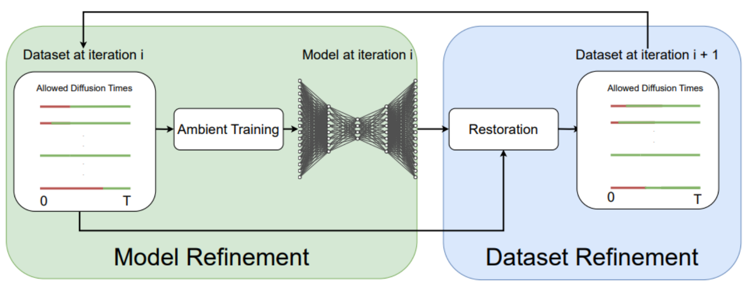

Figure 2: **Illustration of the Ambient Dataloops framework.** At each loop, we are given points that can be used to train the diffusion model at certain noise levels. We train a model on this noisy dataset using Ambient Diffusion (green), and then we use it to improve the dataset through posterior sampling (blue).

We propose a dataset-model co-evolution process, termed **Ambient Dataloops**. At each iteration of this process, we start with a noisy dataset, we use it to train a diffusion model, and then we use the trained model to **gradually** denoise the original dataset. We illustrate some results of this process for a text-conditional model in Figure 1. We avoid catastrophic, self-consuming loops, observed in prior works (Alemohammad et al., 2024a; Shumailov et al., 2024; Hataya et al., 2023; Martínez et al., 2023; Padmakumar & He, 2024; Seddik et al., 2024; Dohmatob et al., 2024) when training on self-generated outputs, by only slightly denoising the dataset each time and by performing corruption-aware diffusion training (e.g. as in Ambient Diffusion (Daras et al., 2025c,b, 2023)). The latter is used to account for errors that happen during the denoising process of the previous round and avoid propagating these errors to the next iteration. Experimentally, Ambient Dataloops consistently outperforms prior work on learning from corrupted data in both controlled settings, as well as in real datasets, including text-conditional models trained on dozens of millions of samples and generative models for protein structures. We further provide theoretical justification for the potential effectiveness of the approach in settings where the initial score estimation is sufficiently accurate.

2 Background and Related Work

Diffusion Models. Diffusion modeling (Sohl-Dickstein et al., 2015; Ho et al., 2020; Song & Ermon, 2019; Song et al., 2021) is one of the most prominent frameworks for learning high-dimensional, complex, continuous distributions. The main algorithmic idea is to consider not only the target density, which we will denote with p_0, but a family of intermediate distributions,

$p_t = p_0 \circledast \mathcal{N}(0, \sigma(t)^2 I)$, where $\sigma(t)$ is an increasing function and t is a continuous variable in $[0, T]$ (for some big constant T) representing the diffusion time. We denote with X_0 the R.V. sampled according to the target density p_0 and similarly $X_t = X_0 + \sigma(t)Z,\ Z \sim \mathcal{N}(0, \sigma(t)^2 I)$ the R.V. sampled according to p_t. During training, the object of interest is the best l_2 denoiser for each one of these intermediate densities, i.e. the conditional expectation of the clean sample given a noisy observation, $\mathbb{E}[X_0|X_t = \cdot]$. The latter is typically optimized with the following objective:

$$J(\theta) = \mathbb{E}_{t \in \mathcal{U}[0,T]} \mathbb{E}_{X_0} \mathbb{E}_{X_t|X_0,t} \left[||h_\theta(X_t, t) - X_0||^2 \right]. \tag{1}$$

For a sufficiently rich parametrization family, the minimizer of this objective is indeed the conditional expectation, i.e. $h_{\theta^*}(\cdot, t) = \mathbb{E}[X_0|X_t = \cdot]$. The latter is connected to the score-function $\nabla \log p_t(\cdot)$ through Tweedie's formula (Tweedie, 1957; Efron, 2011) and it can be used to sample according to a diffusion process (Song et al., 2021; Anderson, 1982).

Finite datasets and imperfect data. In practice, we don't have access to infinite samples from p_0 but to a finite number, denote n_1. When n_1 is small, diffusion models often memorize their training set and learn the empirical distribution $\hat{p}_0$ (Shah et al., 2025; Daras et al., 2024; Somepalli et al., 2023a,b; Carlini et al., 2023; Kamb & Ganguli, 2025; Kadkhodaie et al., 2024).

One way to increase the sample size and improve generalization is to incorporate low-quality or out-of-distribution data that is usually cheaper and more widely available. This occurs naturally in many datasets or can be collected (e.g. data scraping, synthetic data from other models, etc). To avoid hurting the generation quality or biasing the distribution, it is crucial to account for the corruption of this additional data during the training of the diffusion model. Over the past few years, there have been numerous proposed methods for training generative models with imperfect data (Bora et al., 2018; Daras et al., 2023, 2024, 2025a,c,b; Aali et al., 2023, 2025; Lu et al., 2025; Kelkar et al., 2024; Rozet et al., 2024; Bai et al., 2025; Zhang et al., 2025; Tewari et al., 2023; Liu et al., 2025; Alemohammad et al., 2024b). The majority of these works make some assumption about the nature of the degradation in the given data, which is limiting if we want to apply these datasets to Web-scale real datasets that have samples of various qualities and unknown corruption types.

Daras et al. (2025b,c) propose an approach for dealing with data of various qualities without an explicit degradation model. The central idea is that the distance between any two distributions, p_0 and q_0, contracts with the introduction of noise. In this work, q_0 is the distribution obtained by sampling from p_0 but via an unknown noisy measurement process. For a sufficiently high amount of noise, t_n, the distributions p_{t_n} and q_{t_n} approximate well each other. Hence, for noise levels $t \geq t_n$, we can use samples from a low-quality or out-of-distribution data-source q_0 to increase the pool size of available data for a small distribution bias penalty. Daras et al. (2025c) analyze this bias-variance trade-off and provide rigorous ways for deciding the threshold t_n beyond which it is beneficial to incorporate q_0 data. After annotation, each sample from $Y_0 \sim q_0$ is mapped to its noisy version Y_{t_n} and the problem amounts to training a diffusion with a mixture of clean data (from p_0) and samples corrupted with additive Gaussian noise (that are well approximated as coming from p_{t_n}).

The reduction of the problem to the additive noise case enables the leveraging of well-developed statistical tools for learning from noisy data (Stein, 1981; Lehtinen et al., 2018; Moran et al., 2020; Daras et al., 2024, 2025a). In particular, it is possible to learn the conditional expectation of the clean samples with noisy targets. In the most general form, we are given access to a dataset $\mathcal{D}$ where each sample has a known noise level t_i and can be used for diffusion times in $[t_i, T]$. The two extremes are $t_i = 0$ (clean sample, used everywhere) and $t_i = T$ (filtering, the sample is not used at all). Daras et al. (2024) establish that for $\alpha(t, t_i) = \frac{\sigma^2(t) - \sigma^2(t_i)}{\sigma^2(t)}$, given enough data, the following objective has the same minimizer as equation 1, but it does so without having access to clean targets:

$$J_{\text{ambient-o}}(\theta) = \mathbb{E}_{t \in \mathcal{U}[0,T]} \sum_{i : t_i < t} \mathbb{E}_{x_t | x_{t_i}} \left[||\alpha(t, t_i) h_\theta(x_t, t) + (1 - \alpha(t, t_i)) x_t - x_{t_i}||^2 \right], \tag{2}$$

3 Method

Problem Setting. We study exactly the same problem as Daras et al. (2025c,b,a, 2024); in particular, we assume that we have access to a dataset of samples $\mathcal{D} = \{(x_{t_i}, t_i)\}_{i=1}^N$ where each sample x_{t_i} is (at least approximated as) being sampled from a density p_{t_i}. As explained in Section 2, this dataset is typically formed by starting with a dataset that contains some clean samples and some samples of unknown types and then adding the appropriate amount of noise to the corrupted samples to make them look approximately as clean samples corrupted with additive noise. In Section 5, we experiment with such transformed datasets, but in this paper, we do not study the details of how this transformation has been performed and instead use the resulting datasets as our starting point for our method. We refer the interested reader to (Daras et al., 2025c) for more details about how this initial reduction from arbitrary degradations to the additive Gaussian noise case can be performed.

Algorithm. Our method is summarized in Figure 2. It iterates between two steps, for $l = 1, \ldots$:

- ◇ **Model Training.** At this step, we take the training set $\mathcal{D}^{(l-1)}$ and then we train a new model on this dataset. Since the dataset has noisy data, we use the training objective of Equation 2. This is the standard step performed in prior work, e.g., see (Daras et al., 2025c,b,a, 2024).
- ◇ **Dataset Restoration.** At the end of the model training, we have a model $h_{\theta^{(l)}}$. Our method uses this network to *denoise* the *original dataset*. In particular, we perform posterior sampling $X_{t_i/2^l} \sim p_{\theta^{(l)}, t_i/2^l}(\cdot | x_{t_i}, t_i)$ and add $(X_{t_i/2^l}, t_i/2^l)$ to a new dataset $\mathcal{D}^{(l)}$. Simply put, this procedure synthetically reduces the noise level of the original dataset by denoising from t to $t/2^l$ using the best prior model available at iteration l. The constant 2 effectively controls the amount of progress we expect each iteration of this algorithm to achieve, and in practice, it can be tuned as a hyperparameter.

A complete description of the algorithm is provided in Algorithm 1.

Algorithm 1 Ambient Dataloops Training Algorithm.

Require: dataset $\mathcal{D}^{(0)} = \{(x_{t_i}, t_i)\}_{i=1}^{N}$, noise scheduling $\sigma(t)$, batch size B, diffusion time T, number of loops L, random weights $\theta^{(0)}$.

for $l \in [1, L]$ **do** ▷ A new loop starts.
  $\theta^{(l)} \leftarrow \theta^{(l-1)}$ ▷ Initialize from the weights of the previous round (finetuning).
  while not converged **do** ▷ A new training starts.
    $t_{s_1}, ..., t_{s_B} \leftarrow$ Sample uniformly B times in $[0, T]$
    $(x_{\bar{t_1}}, \bar{t_1}), ..., (x_{\bar{t_B}}, \bar{t_B}) \leftarrow$ Sample eligible points for times $t_{s_1}, ..., t_{s_B}$ from $\mathcal{D}^{(l-1)}$
    loss $\leftarrow 0$ ▷ Initialize loss.
    for $(x_{\bar{t_i}}, \bar{t_i}, t_{s_i}) \in (x_{\bar{t_1}}, \bar{t_1}, t_{s_1}), ..., (x_{\bar{t_B}}, \bar{t_B}, t_{s_B})$ **do**
      $\epsilon \sim \mathcal{N}(0, I)$ ▷ Sample noise.
      $x_{t_{s_i}} \leftarrow x_{\bar{t_i}} + \sqrt{\sigma^2(t_{s_i}) - \sigma^2(\bar{t_i})}\epsilon$ ▷ Add additional noise.
      $\alpha(t_{s_i}, \bar{t_i}) \leftarrow \frac{\sigma^2(t_{s_i}) - \sigma^2(\bar{t_i})}{\sigma^2(t_{s_i})}$,
      $w(t_{s_i}, \bar{t_i}) \leftarrow \frac{\sigma^4(t_{s_i})}{\left(\sigma^2(t_{s_i}) - \sigma^2(\bar{t_i})\right)^2}$. ▷ Loss reweighting.
      loss $\leftarrow$ loss + $w(t_{s_i}, \bar{t_i}) \left|\left|\alpha(t, t_i) h_{\theta^{(l)}}(x_{t_{s_i}}, t_{s_i}) + (1 - \alpha(t_{s_i}, \bar{t_i}))x_{t_{s_i}} - x_{\bar{t_i}}\right|\right|^2$
    end for
    loss $\leftarrow \frac{\text{loss}}{B}$ ▷ Compute average loss.
    $\theta^{(l)} \leftarrow \theta^{(l)} - \eta \nabla_{\theta^{(l)}}$loss ▷ Update network parameters via backpropagation.
  end while
  $\mathcal{D}^{(l)} = \emptyset$
  for $(x_{t_i}, t_i) \in \mathcal{D}^{(0)}$ **do** ▷ A new restoration cycle starts.
    $x_{t_i/2^l} \sim p_{\theta^{(l)}, t_i/2^l}(\cdot | x_{t_i}, t_i)$ ▷ Perform posterior sampling from t_i to $t_i/2^l$.
    $\mathcal{D}^{(l)} \leftarrow \mathcal{D}^{(l)} \cup (x_{t_i/2^l}, t_i/2^l)$ ▷ Add restored point to dataset.
  end for
end for

Discussion. The crux of this algorithm is dataset refinement; at each loop, we use the best model we have to improve the dataset by reducing the amount of noise in its samples. The resulting dataset can be used for a new training and so forth. As we run more loops, the model becomes better, and hence we take bigger denoising steps. We provide an overview of the approach in Figure 2.

Potential limitations. The idea of dataset refinement, despite being natural, has three issues. First, it seems to be violating the data processing inequality; information cannot be created out of thin air, and hence any processing of the original data cannot have more information for the underlying distribution than the original dataset. While this is true, it is important to consider that the first training might be suboptimal due to failures of the optimization process (e.g., gradient descent getting stuck in a local minimum). Hence, dataset refinement can be thought of as a reorganization of the original information in a way that facilitates learning and creates a better optimization landscape.

Another challenge for our method is that we train on synthetic data. Several recent works have shown that naive training on synthetic data leads to catastrophic self-confusing loops and mode collapse (Alemohammad et al., 2024a; Shumailov et al., 2024; Hataya et al., 2023; Martínez et al., 2023; Padmakumar & He, 2024; Seddik et al., 2024; Dohmatob et al., 2024). Our key idea to get around this issue is to treat the restorations as *noisy* data as well, just at a smaller noise level compared to where the restoration started. In particular, we do not run the full posterior sampling algorithm; we early stop the generation process at time $t_i/2^l$ at each round l. Prior work has shown that the catastrophic self-consuming loops can be avoided using a *verifier* that assesses the quality of the generations (Ferbach et al., 2024; Feng et al., 2024; Zhang et al., 2024). The gradual denoising and the finite number of rounds in our algorithm have a similar effect. Tuning the number of rounds wisely prevents the model from attempting to denoise the dataset at a level beyond what's possible using the available training set. Naturally, tuning this parameter in practice is not straightforward, and we provide ablations of miscalibration in our experiments.

The last issue associated with our approach has to do with the associated computational requirements. At each round, we have to restore the whole dataset and then fine-tune the model, leading to an increase in the training cost. Indeed, this method is useful when data, not compute, is the bottleneck. Our framework trains to extract as much utility as possible from a given training set; if there is more data available, it is always better to perform training updates on it as fresh samples reveal more about the underlying distribution (Goyal et al., 2024).

4 Theoretical Modeling

In this section, we study the theoretical aspects of the proposed method. We consider a stylized setting and version of the algorithm, arguing that if the score function is sufficiently well-approximated after the first iteration, then performing a *dataset refinement* step can improve the estimation error.

Setting. For the purposes of the theoretical analysis, we adopt the theoretical setting from Ambient Omni (Daras et al., 2025c), and identify conditions under which *dataset looping* is beneficial.

In the description of our method, we assumed that we have access to a dataset $\mathcal{D}_0 = \{(x_{t_i}, t_i)\}_{i=1}^N$, where each datapoint comes with a threshold time t_i indicating that we will use it to estimate scores for diffusion times $t \geq t_i$. As discussed earlier, the way those samples and associated threshold times came about is as follows: Some are samples from the target distribution p_0, and all these samples are assigned a threshold time 0. Then there are samples from distributions different from p_0. If some sample was sampled from some distribution q_0, we would add to it noise sampled from $\mathcal{N}(0, \sigma_{t_i}^2 I)$ and assigned to the noised sample threshold time t_i, where the choice of t_i depends on the distance between p_0 and q_0. The choice would be such that p_{t_i} and q_{t_i} are sufficiently close that for $t \geq t_i$ we prefer to include this sample in estimating scores versus not using it. Choosing those times correctly is complex, but the theoretical analysis in Ambient Omni provides us guidance for how to choose these times, in the case where all samples either come from p_0 or from q_0, as described below. So let us stick to this case for our analysis here as well.

In particular, we are given n_1 samples from a target distribution p_0 that we want to learn to generate. We assume that p_0 is supported on $[0, 1]$ and is λ_1-Lipschitz. We are also given n_2 samples from a distribution q_0, which is not the target distribution, and may have some distance from p_0. We assume that q_0 is λ_2-Lipschitz. We want to train a diffusion model to sample p_0, so we need to learn the score functions of all distributions $p_t = p_0 \circledast \mathcal{N}(0, \sigma_t^2 I)$. Given n_1 i.i.d. samples from p_0 we can create n_1 i.i.d. samples from p_t. Given our n_2 i.i.d. samples from q_0 we can also create n_2 i.i.d. samples from $q_t = q_0 \circledast \mathcal{N}(0, \sigma_t^2 I)$, but again q_t is different from p_t. The observation that Daras et al. (2025c) leverage is that q_t is closer to p_t than q_0 is to p_0 because convolution with a Gaussian distribution contracts distances.

Because of this contraction, it could be that for sufficiently large t's (a.k.a. σ_t's), we are better off including the n_2 (biased) samples from q_t to estimate p_t rather than only using the unbiased samples from p_t. Indeed this is what is shown by Daras et al. (2025c) in Ambient Omni, as discussed below.

Prior results. For any diffusion time t, Daras et al. (2025c) compare the accuracy attained by the following algorithms:

- **Algorithm 1**: Use the n_1 samples from p_t and estimate p_t using denoising diffusion training.
- **Algorithm 2**: Use $(n_1 + n_2)$ samples from the mixutre density $\tilde{p}_t = \frac{n_1}{n_1+n_2} p_t + \frac{n_2}{n_1+n_2} q_t$ and estimate p_t using denoising diffusion training by pretending that all training samples are from p_t.

Using a connection between diffusion training and kernel density estimation, Daras et al. (2025c) show that, with probability $(1 - \delta)$, it is better to use Algorithm 2 over Algorithm 1 for times t:

$$\frac{1}{(n_1+n_2)} + \frac{1}{\sigma_t^2(n_1+n_2)} + \sqrt{\frac{\log(n_1+n_2) + \log(1 \vee \frac{n_1}{n_1+n_2}\lambda_1 + \frac{n_2}{n_1+n_2}\lambda_2) + \log 2/\delta}{\sigma_t^2(n_1+n_2)}}$$
$$+ \frac{n_2}{\sigma_t(n_1+n_2)} \mathrm{d}_{\mathrm{TV}}(p_0, q_0) \leq \frac{1}{n_1} + \frac{1}{\sigma_t^2 n_1} + \sqrt{\frac{\log n_1 + \log(1 \vee \lambda_1) + \log 2/\delta}{\sigma_t^2 n_1}}. \tag{3}$$

Improved results through looping. The theory of Ambient Omni compared (1) using only samples from the true distribution p_t (Algorithm 1), or (2) using samples from $\tilde{p}_t$ which is a mixture of the true distribution p_t and the biased distribution q_t (Algorithm 2). However, there are more possibilities for learning. Our datalooping algorithm motivates the following alternate algorithm:

- **Algorithm 3**: Transform samples from q_t using a (potentially stochastic and learned) mapping function f. This defines the push-forward measure $\bar{q}_t = f \sharp q_t$. Then, learn using $(n_1 + n_2)$ samples from the distribution: $\tilde{\tilde{p}}_t = \frac{n_1}{n_1+n_2} p_t + \frac{n_2}{n_1+n_2} \bar{q}_t$.

Notice that Algorithm 3 is a generalization of Algorithm 2, as the latter is recovered using the identity transformation function. Denote by $p_{t,\text{approx}}^{(L)}$ the approximate density estimated by Algorithm L, for $L = 1, 2, 3$. Using the same connection between diffusion model training and Gaussian kernel density estimation, it is straightforward to show the following lemma:

Lemma 1 (Contractive transformations lead to better learning)**.** *If the mapping function f contracts the TV distance with respect to the underlying true density p_t, i.e., if for any density ϕ it holds that:*

$$\mathrm{d}_{\mathrm{TV}}(f \sharp \phi, p_t) \leq \mathrm{d}_{\mathrm{TV}}(\phi, p_t), \tag{4}$$

then, in all cases where Algorithm 2 is preferable to Algorithm 1 (e.g., for cases that Eq. 3 holds), Algorithm 3 is weakly preferable to Algorithm 2, and it is strictly preferable if Eq. 4 is strict.

The lemma's statement is intuitive; if we have a way to "correct" the samples from the out-of-distribution density q_t, we should be able to achieve a better approximation to p_t if we were to correct them versus using them as is. A related work (Gillman et al., 2024) studies the implications of having an idealized corrector function for learning from bad data (in their case, synthetic data) and establishes asymptotic convergence to the underlying distribution. Our result is similar in spirit, but the analysis is done for the implicit kernel-density estimation that diffusion modeling obtains.

With the above observations in place, let us identify conditions under which an idealized variant of Algorithm 1 would reduce the estimation error after one iteration of dataset refinement. In particular, suppose that all the correct scores were known and we perform posterior sampling of $X_{t'}$ given X_t for all $X_t \sim q_t$ and some $t' < t$. This would correspond to running the reverse diffusion process (Anderson, 1982; Oksendal, 2013) initializing at X_t at time t down to time t':

$$dX_t = -\nabla \log p_t(X_t) dt + \sqrt{2} \mathrm{d}B_t, \tag{5}$$

where B_t is the standard Wiener process. Suppose that $f_{t,t'}$ is the resulting randomized map from X_t to $X_{t'}$. Under appropriate assumptions on the p_t's, the sampled distribution $f_{t,t'} \# q_t$ is closer to $p_{t'}$ compared to $q_{t'}$. Thus, Algorithm 3, using samples from $f_{t,t'} \# q_t$ would have better estimation error compared Algorithm 2 using samples from $q_{t'}$ per Lemma 1.

Learning Errors. The above describes what the framework would achieve in an idealized scenario where we have access to the true scores. The issue is that in practice, we cannot run Eq. 5 since we only have an approximation to the true score. To wit, our looping framework *approximates* the score function with the *best estimator using the current data*. In particular, for times t for which Algorithm 2 is preferred to Algorithm 1, the estimation we have from the first round is:

$$\nabla \log p^{(2)}_{t,\text{approx}}(x) = \frac{1}{(n_1+n_2)\sqrt{2\pi\sigma_t^2}} \left(\sum_{i=1}^{n_1} w(x, x_i)(x - x_i) + \sum_{i=1}^{n_2} w(x, x_i')(x - x_i) \right), \quad (6)$$

where $w(x, y) = \mathcal{N}(x; \mu = y, \sigma = \sigma_t^2)$, and $\{x_i\}_i$ are the samples from p_t while $\{x_i'\}_i$ are the samples from q_t. This score only approximates the desired one, $\nabla \log p_t$. Due to this estimation error, running the Langevin Diffusion process of Eq. 5 would perform worse in terms of contraction towards $p_{t'}$. In practice, our experiments show that our estimates are sufficiently good estimates of the score function, and hence Algorithm 3 obtains faster rates of convergence than Algorithms 1 or 2.

5 Experimental Results

5.1 Controlled experiments with known corruptions

Experimental Setting. We start our experiments by validating our approach in controlled settings. We follow the experimental methodology of the Ambient Omni paper; in particular, we train models on CIFAR-10 by corrupting 90% of the dataset with Gaussian Blur and JPEG compression at various degradation levels while keeping 10% of the dataset intact. We use the parameter σ_B to refer to the standard deviation of the Gaussian kernel used for blurring the dataset images and the parameter q to denote the file size after JPEG compression compared to the original file size.

We compare with the following baselines: **a)** quality-filtering (training only on the clean data), **b)** treating all-data as equal, and, **c)** Ambient Omni (Daras et al., 2025c), which is currently the state-of-the-art for learning diffusion generative models from corrupted data with unknown degradation types. We always initialize our method with the Ambient Omni checkpoints (loop 0). We further directly take the mapping between the low-quality samples (e.g. blurry/JPEG images) and their corresponding noising time (see Section 2) from the work of Daras et al. (2025c), when needed.

Unconditional and Conditional Metrics. We present unconditional FID results for all the baselines and one loop of our method in Table 1 (top). As shown, even a single loop of our proposed method leads to consistent and significant FID improvements up to 17% reduction in FID.

Table 1: Unconditional and conditional results for CIFAR-10 with 90% corrupted and 10% clean data.

Corruption		Filtering	No Filtering	L0 (FID ↓)	L1 (FID ↓)
Blur	$\sigma_B = 0.6$	8.79	11.26	5.34	**5.20**
	$\sigma_B = 0.8$	8.79	28.26	5.98	**5.41**
JPEG	$q = 25$	8.79	91.55	6.34	**5.34**
	$q = 18$	8.79	112.43	6.46	**5.71**

Corruption		Dataset after L0			Dataset after L1		
		LPIPS ↓	MSE ↓	C-FID ↓	LPIPS ↓	MSE ↓	C-FID ↓
Blur	$\sigma_B = 0.6$	0.065	0.745	3.915	**0.063**	**0.742**	**3.863**
	$\sigma_B = 0.8$	0.083	0.895	**4.471**	**0.082**	**0.891**	4.481
JPEG	$q = 25$	0.052	**0.680**	**4.453**	**0.051**	0.681	4.789
	$q = 18$	0.058	**0.719**	**4.740**	**0.057**	0.722	5.260

One benefit of starting our experimental analysis on this controlled setting is that we have the ground truth for the corrupted samples, and hence we can report conditional metrics too. We report conditional FID, LPIPS and MSE. Conditional FID is defined as follows; for each sample (x_{t_i}, t_i) in the dataset we use a given model h_θ to sample from $\bar{X}_0 \sim p_{\theta,0}(\cdot|x_{t_i}, t_i)$, where $p_{\theta,0}(\cdot|x_{t_i}, t_i)$ is the distribution that arises by running the learned reverse process initialized at time $t = t_i$ with the noisy sample x_{t_i}. We then compute the FID between the set sampled with posterior sampling and the reference set. MSE and LPIPS are point-wise restoration metrics and hence it is more meaningful to compute them by measuring the distance of the ground-truth sample to the posterior mean, rather than any random sample from the posterior distribution. In particular, for each sample (x_{t_i}, t_i) in the dataset we use a given model h_θ to estimate with Monte Carlo the posterior mean defined as $\mathbb{E}_{\bar{X}_0 \sim p_{\theta,0}(\cdot|x_{t_i}, t_i)}[\bar{X}_0]$. For a perfectly trained model and ignoring discretization errors, this quantity equals $h_\theta(x_{t_i}, t_i)$, but we use the former quantity to account for learning and sampling errors.

We report our conditional results in Table 1 (bottom). Interestingly, despite the fact that unconditional FID is always better for the model after the loop, this is not always the case for the conditional metrics. A corollary is that if we use the L1 model to restore the dataset, we might yield worse performance compared to stopping after 1 loop. This indeed can happen, and we investigate it in the next paragraph.

Multiple loops and rate of progress. Roughly speaking, there are two reasons that can lead to deterioration in performance. The first has to do with the inherent limit on how much a finite dataset can be denoised reliably. Attempting to go beyond this limit will cause any algorithm to fail. The second reason has to do with the optimization (looping) process, i.e. with *how we reach the denoising limit*. We investigate this extensively in Appendix Table 5. The key takeaway is that being conservative, i.e., doing gradual denoising of the dataset, is optimal if we have the compute budget to afford multiple loops. In particular, for $\sigma_B = 0.6$, doing one loop achieves a conditional FID 3.86 while running 3 loops achieves a record conditional FID 3.29. Both methods achieve comparable unconditional FIDs, but the latter also leads to a better denoised dataset, which comes at the cost of more computation. On the other hand, if we cannot afford running multiple loops, Table 5 suggests that taking a larger denoising step at the single loop we are going to run is optimal.

Other ablations. Beyond the number of loops and the rate of denoising progress, we provide numerous ablations in the Appendix that quantify the role of different aspects of our approach. In particular, Figure 4 shows that the improvements are across all diffusion times, Table 4 shows that there are benefits in sampling multiple times from the posterior, and 3 shows the effect of restoring the dataset of the previous round compared to always restoring the original dataset. The main takeaway is that by carefully tuning parts of the pipeline, we can further boost performance. For example, in the Appendix, we manage to push the unconditional FID for $\sigma_B = 0.6$ on CIFAR from the 5.34 reported in Omni all the way to 4.52. While such improvements are possible, we run the majority of the experiments in the main paper with the simplest variant of our method, as it achieves comparable performance and is far more educational to the reader.

5.2 Experiments with synthetic data and text-to-image models

Having established the effectiveness of the method in controlled settings, we are now ready to test our algorithm in real use cases. In particular, we experiment with text-to-image generative modeling, following the architectural and dataset choices of MicroDiffusion (Sehwag et al., 2025). Sehwag et al. (2025) train a diffusion model from scratch using only 8 GPUs in 2 days. During that training, 4 datasets are used; Conceptual Captions (12M) (Sharma et al., 2018), Segment Anything (11M) (Kirillov et al., 2023), JourneyDB (4.2M) (Sun et al., 2023), and DiffusionDB (10.7M) (Wang et al., 2022). Daras et al. (2025c) noticed that DiffusionDB, despite contributing 28.23% of the dataset samples, contains synthetic images that have significantly lower quality than the rest of the dataset. To account for this, the authors noise the DiffusionDB dataset to level $\sigma_{\text{DiffusionDB}} = 2.0$ and only use it to train for diffusion times $t : \sigma_t \geq 2.0$. This leads to a significant COCO FID improvement compared to using it as clean; FID drops from 12.37 to 10.61.

We now attempt to further improve the performance by taking the model trained by Daras et al. (2025c) to denoise the DiffDB dataset and then train a new model on the denoised set. Consistent with the description of our algorithm in Section 3, we do partial dataset restoration by performing posterior sampling to bring the DiffDB dataset at noise level $\sigma'_{\text{DiffusionDB}} = \sigma_{\text{DiffusionDB}}/2 = 1.0$. We then train the model on this denoised dataset, using the Ambient Diffusion training objective equation 2, as usual. The resulting model achieves further improvements to COCO FID and CLIP-FD score, as shown in Table 2 and scores comparable at GenEval (GPT-4o evaluations) across different categories. Figure 1 shows examples of images from DiffDB and their evolution across our looping process. As seen, the datasets seem to be converging after 1 loop.

Table 2: Quantitative benefits of Ambient Loops on COCO zero-shot generation and GenEval.

Method	COCO (Fidelity & Alignment)		GenEval Benchmark						
	FID-30K (↓)	Clip-FD-30K (↓)	Overall	Single	Two	Counting	Colors	Position	Color attribution
Micro-diffusion	12.37	10.07	0.44	0.97	0.33	0.35	0.82	0.06	0.14
Ambient-o (L0)	10.61	9.40	0.47	0.97	**0.40**	**0.36**	0.82	0.11	0.14
Ambient Loops (L1)	**10.06**	**8.83**	**0.47**	**0.97**	0.38	0.35	0.78	**0.11**	**0.19**

5.3 De-novo protein design

Introduction. For this final part of our experimental evaluation, we switch modality and target structural protein design. This problem is significant because accurate de novo protein structure models can result in improved designs for new vaccines, therapeutics, and enzymes. The problem is also well-suited for our Ambient Dataloops framework, as techniques for determining the atomistic resolution of molecular protein structures (such as X-ray crystallography) are inherently noisy. On top of that, acquiring samples through such techniques requires domain expertise and significant resources and hence the available datasets, such as the Protein Data Bank, are of limited size. To enrich the dataset, recent state-of-the-art models for protein backbones are trained on synthetic data from AlphaFold, which once again contain corrupted samples due to learning errors in folding.

Setting. Daras et al. (2025b) applied the Ambient Omni (Daras et al., 2025c) framework to train a generative model for protein backbones. We use the same dataset, architectural, and training procedures as in (Daras et al., 2025b) to demonstrate that looping can improve performance in domains beyond Computer Vision. In particular, we start with the dataset of Daras et al. (2025b) that contains 90,250 structurally unique proteins from the AlphaFold Data Bank (AFDB) dataset, with a maximum length of 256 residues. To find the associated noise level of the dataset we follow once again the experimental protocol of the authors, which is to map proteins to diffusion times according to AlphaFold's self-reported confidence for the predicted structure as given by the pLDDT score. We then use the Ambient Proteins (Daras et al., 2025b) model to denoise its training set and we start a new training run on the denoised dataset. One example of such a denoising is given in Figure 3b. In agreement with the rest of the paper, we also treat the denoised dataset as noisy, but at a lower noise level. In this particular domain, we use the existing pLDDT to diffusion time mapping from Ambient Proteins (Daras et al., 2025b) and we treat the denoised predictions as increasing the pLDDT (synthetically) by 3 points in each denoised sample. We arrived at this value after ablating different pLDDT adjustments that led to inferior results. To assess the quality of the trained models, we use the two most established metrics in the field: Designability and Diversity. There is a trade-off between the two metrics that defines a Pareto frontier in the joint space.

Results. Just one loop of our procedure is enough to achieve a new Pareto point, as shown in Figure 3a. In particular, we trade 0.2% decrease in designability for a 14.3% increase in diversity, significantly expanding the creativity boundaries of the loop 0 model for the same inference parameters. Both models dominate in the Pareto frontier over other baselines showing both the promise of degradation-aware diffusion training and the potential of datalooping to enhance the generative capabilities for protein design. While our protein evaluation is preliminary and the results need to be verified in the wet lab, the metrics suggest that datalooping could be useful for scientific domains.

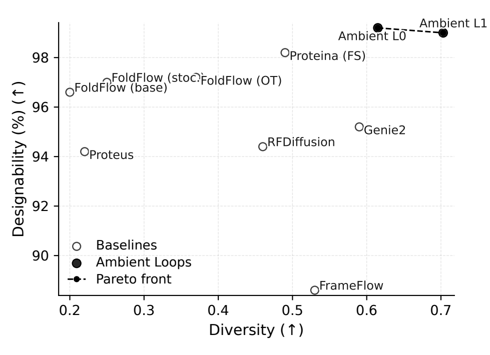

(a) Designability-Diversity trade-off for de novo design of protein backbones. Training with Ambient Proteins dominates the Pareto frontier. One loop of our framework achieves a 14.3% increase in diversity for a minor 0.2% in designability.

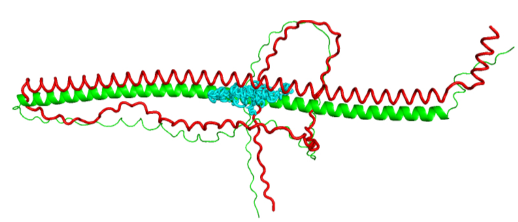

(b) Example of our dataset refinement procedure. An initial low pLDDT protein, denoted with green, is noised to a certain level, giving the shape in cyan. We initialize the reverse process with the cyan sample, and we sample the red point from the posterior.

Figure 3: (a) Pareto frontier for protein backbone design. (b) Example point refinement procedure.

6 Conclusions and Future Work

We introduced Ambient Dataloops, a framework that enables better learning of the underlying data distribution by refining the dataset together with the model being trained. We experimentally validated our approach in various settings, ranging from controlled experiments to text-conditional generative models and de novo protein design settings. This algorithm paves the way for denoising scientific datasets where sample quality naturally varies and it has the potential to improve not only generative models but also supervised models optimized for downstream applications.

Acknowledgments

This research has been supported by NSF Awards CCF-1901292, ONR grants N00014-25-1-2116, N00014-25-1-2296, a Simons Investigator Award, and the Simons Collaboration on the Theory of Algorithmic Fairness. The experiments were run on the Vista GPU Cluster through the Center for Generative AI (CGAI) and the Texas Advanced Computing Center (TACC) at UT Austin. Adrián Rodríguez-Muñoz is supported by the La Caixa Fellowship (LCF/BQ/EU22/11930084).

References

Asad Aali, Marius Arvinte, Sidharth Kumar, and Jonathan I. Tamir. Solving inverse problems with score-based generative priors learned from noisy data. In *2023 57th Asilomar Conference on Signals, Systems, and Computers*, pp. 837–843. IEEE, October 2023. doi: 10.1109/ieeeconf59524.2023.10477042. URL `http://dx.doi.org/10.1109/IEEECONF59524.2023.10477042`.

Asad Aali, Giannis Daras, Brett Levac, Sidharth Kumar, Alex Dimakis, and Jon Tamir. Ambient diffusion posterior sampling: Solving inverse problems with diffusion models trained on corrupted data. In *The Thirteenth International Conference on Learning Representations*, 2025. URL `https://openreview.net/forum?id=qeXcMutEZY`.

Sina Alemohammad, Josue Casco-Rodriguez, Lorenzo Luzi, Ahmed Imtiaz Humayun, Hossein Babaei, Daniel LeJeune, Ali Siahkoohi, and Richard G Baraniuk. Self-consuming generative models go mad. International Conference on Learning Representations (ICLR), 2024a.

Sina Alemohammad, Ahmed Imtiaz Humayun, Shruti Agarwal, John Collomosse, and Richard Baraniuk. Self-improving diffusion models with synthetic data. *arXiv preprint arXiv:2408.16333*, 2024b.

Brian DO Anderson. Reverse-time diffusion equation models. *Stochastic Processes and their Applications*, 12(3):313–326, 1982.

Weimin Bai, Yifei Wang, Wenzheng Chen, and He Sun. An expectation-maximization algorithm for training clean diffusion models from corrupted observations. In *Proceedings of the 38th International Conference on Neural Information Processing Systems*, NIPS '24, Red Hook, NY, USA, 2025. Curran Associates Inc. ISBN 9798331314385.

Kevin Black, Michael Janner, Yilun Du, Ilya Kostrikov, and Sergey Levine. Training diffusion models with reinforcement learning. *arXiv preprint arXiv:2305.13301*, 2023.

Ashish Bora, Eric Price, and Alexandros G. Dimakis. AmbientGAN: Generative models from lossy measurements. In *International Conference on Learning Representations*, 2018. URL `https://openreview.net/forum?id=Hy7fDog0b`.

Nicholas Carlini, Jamie Hayes, Milad Nasr, Matthew Jagielski, Vikash Sehwag, Florian Tramèr, Borja Balle, Daphne Ippolito, and Eric Wallace. Extracting training data from diffusion models. In *Proceedings of the 32nd USENIX Conference on Security Symposium*, SEC '23, USA, 2023. USENIX Association. ISBN 978-1-939133-37-3.

Giannis Daras, Kulin Shah, Yuval Dagan, Aravind Gollakota, Alex Dimakis, and Adam Klivans. Ambient diffusion: Learning clean distributions from corrupted data. In A. Oh, T. Naumann, A. Globerson, K. Saenko, M. Hardt, and S. Levine (eds.), *Advances in*

Neural Information Processing Systems, volume 36, pp. 288–313. Curran Associates, Inc., 2023. URL https://proceedings.neurips.cc/paper_files/paper/2023/file/012af729c5d14d279581fc8a5db975a1-Paper-Conference.pdf.

Giannis Daras, Alexandros G. Dimakis, and Constantinos Daskalakis. Consistent diffusion meets tweedie: training exact ambient diffusion models with noisy data. In *Proceedings of the 41st International Conference on Machine Learning*, ICML'24. JMLR.org, 2024.

Giannis Daras, Yeshwanth Cherapanamjeri, and Constantinos Costis Daskalakis. How much is a noisy image worth? data scaling laws for ambient diffusion. In *The Thirteenth International Conference on Learning Representations*, 2025a. URL https://openreview.net/forum?id=qZwtPEw2qN.

Giannis Daras, Jeffrey Ouyang-Zhang, Krithika Ravishankar, William Daspit, Costis Daskalakis, Qiang Liu, Adam Klivans, and Daniel J. Diaz. Ambient proteins: Training diffusion models on low quality structures. *bioRxiv*, 2025b. doi: 10.1101/2025.07.03.663105. URL https://www.biorxiv.org/content/early/2025/07/05/2025.07.03.663105.

Giannis Daras, Adrian Rodriguez-Munoz, Adam Klivans, Antonio Torralba, and Constantinos Daskalakis. Ambient diffusion omni: Training good models with bad data. *arXiv preprint arXiv:2506.10038*, 2025c.

Justas Dauparas, Ivan Anishchenko, Nathaniel Bennett, Hua Bai, Robert J Ragotte, Lukas F Milles, Basile IM Wicky, Alexis Courbet, Rob J de Haas, Neville Bethel, et al. Robust deep learning–based protein sequence design using proteinmpnn. *Science*, 378(6615):49–56, 2022.

Elvis Dohmatob, Yunzhen Feng, Pu Yang, Francois Charton, and Julia Kempe. A tale of tails: Model collapse as a change of scaling laws. *arXiv preprint arXiv:2402.07043*, 2024.

Carles Domingo-Enrich, Michal Drozdzal, Brian Karrer, and Ricky TQ Chen. Adjoint matching: Fine-tuning flow and diffusion generative models with memoryless stochastic optimal control. *arXiv preprint arXiv:2409.08861*, 2024.

Bradley Efron. Tweedie's formula and selection bias. *Journal of the American Statistical Association*, 106(496):1602–1614, 2011.

Yunzhen Feng, Elvis Dohmatob, Pu Yang, Francois Charton, and Julia Kempe. Beyond model collapse: Scaling up with synthesized data requires verification. *arXiv preprint arXiv:2406.07515*, 2024.

Damien Ferbach, Quentin Bertrand, Avishek Joey Bose, and Gauthier Gidel. Self-consuming generative models with curated data provably optimize human preferences. *arXiv preprint arXiv:2407.09499*, 2024.

Samir Yitzhak Gadre, Gabriel Ilharco, Alex Fang, Jonathan Hayase, Georgios Smyrnis, Thao Nguyen, Ryan Marten, Mitchell Wortsman, Dhruba Ghosh, Jieyu Zhang, Eyal Orgad, Rahim Entezari, Giannis Daras, Sarah M Pratt, Vivek Ramanujan, Yonatan Bitton, Kalyani Marathe, Stephen Mussmann, Richard Vencu, Mehdi Cherti, Ranjay Krishna, Pang Wei Koh, Olga Saukh, Alexander Ratner, Shuran Song, Hannaneh Hajishirzi, Ali Farhadi, Romain Beaumont, Sewoong Oh, Alex Dimakis, Jenia Jitsev, Yair Carmon, Vaishaal Shankar, and Ludwig Schmidt. Datacomp: In search of the next generation of multimodal datasets. In *Thirty-seventh Conference on Neural Information Processing Systems Datasets and Benchmarks Track*, 2023. URL https://openreview.net/forum?id=dVaWCDMBof.

Nate Gillman, Michael Freeman, Daksh Aggarwal, Chia-Hong Hsu, Calvin Luo, Yonglong Tian, and Chen Sun. Self-correcting self-consuming loops for generative model training. *arXiv preprint arXiv:2402.07087*, 2024.

Sachin Goyal, Pratyush Maini, Zachary C Lipton, Aditi Raghunathan, and J Zico Kolter. Scaling laws for data filtering–data curation cannot be compute agnostic. In *Proceedings of the IEEE/CVF Conference on Computer Vision and Pattern Recognition*, pp. 22702–22711, 2024.

Ryuichiro Hataya, Han Bao, and Hiromi Arai. Will large-scale generative models corrupt future datasets? In *Proceedings of the IEEE/CVF International Conference on Computer Vision*, pp. 20555–20565, 2023.

Tom Henighan, Jared Kaplan, Mor Katz, Mark Chen, Christopher Hesse, Jacob Jackson, Heewoo Jun, Tom B Brown, Prafulla Dhariwal, Scott Gray, et al. Scaling laws for autoregressive generative modeling. *arXiv preprint arXiv:2010.14701*, 2020.

Jonathan Ho, Ajay Jain, and Pieter Abbeel. Denoising diffusion probabilistic models. In *Proceedings of the 34th International Conference on Neural Information Processing Systems*, NIPS '20, Red Hook, NY, USA, 2020. Curran Associates Inc. ISBN 9781713829546.

Jordan Hoffmann, Sebastian Borgeaud, Arthur Mensch, Elena Buchatskaya, Trevor Cai, Eliza Rutherford, Diego de Las Casas, Lisa Anne Hendricks, Johannes Welbl, Aidan Clark, et al. Training compute-optimal large language models (2022). *arXiv preprint arXiv:2203.15556*, 2022.

Zahra Kadkhodaie, Florentin Guth, Eero P Simoncelli, and Stéphane Mallat. Generalization in diffusion models arises from geometry-adaptive harmonic representations. In *The Twelfth International Conference on Learning Representations*, 2024. URL `https://openreview.net/forum?id=ANvmVS2Yr0`.

Mason Kamb and Surya Ganguli. An analytic theory of creativity in convolutional diffusion models. In *Forty-second International Conference on Machine Learning*, 2025. URL `https://openreview.net/forum?id=ilpL2qACla`.

Jared Kaplan, Sam McCandlish, Tom Henighan, Tom B Brown, Benjamin Chess, Rewon Child, Scott Gray, Alec Radford, Jeffrey Wu, and Dario Amodei. Scaling laws for neural language models. *arXiv preprint arXiv:2001.08361*, 2020.

Varun A. Kelkar, Rucha Deshpande, Arindam Banerjee, and Mark Anastasio. Ambientflow: Invertible generative models from incomplete, noisy measurements. *Transactions on Machine Learning Research*, 2024. ISSN 2835-8856. URL `https://openreview.net/forum?id=txpYITR8oa`.

Alexander Kirillov, Eric Mintun, Nikhila Ravi, Hanzi Mao, Chloe Rolland, Laura Gustafson, Tete Xiao, Spencer Whitehead, Alexander C. Berg, Wan-Yen Lo, Piotr Dollár, and Ross Girshick. Segment anything, 2023. URL `https://arxiv.org/abs/2304.02643`.

Jaakko Lehtinen, Jacob Munkberg, Jon Hasselgren, Samuli Laine, Tero Karras, Miika Aittala, and Timo Aila. Noise2noise: Learning image restoration without clean data. *arXiv preprint arXiv:1803.04189*, 2018.

Jeffrey Li, Alex Fang, Georgios Smyrnis, Maor Ivgi, Matt Jordan, Samir Yitzhak Gadre, Hritik Bansal, Etash Kumar Guha, Sedrick Keh, Kushal Arora, Saurabh Garg, Rui Xin, Niklas Muennighoff, Reinhard Heckel, Jean Mercat, Mayee F Chen, Suchin Gururangan, Mitchell Wortsman, Alon Albalak, Yonatan Bitton, Marianna Nezhurina, Amro Kamal Mohamed Abbas, Cheng-Yu Hsieh, Dhruba Ghosh, Joshua P Gardner, Maciej Kilian, Hanlin Zhang, Rulin Shao, Sarah M Pratt, Sunny Sanyal, Gabriel Ilharco, Giannis Daras, Kalyani Marathe, Aaron Gokaslan, Jieyu Zhang, Khyathi Chandu, Thao Nguyen, Igor Vasiljevic, Sham M. Kakade, Shuran Song, Sujay Sanghavi, Fartash Faghri, Sewoong Oh, Luke Zettlemoyer, Kyle Lo, Alaaeldin El-Nouby, Hadi Pouransari, Alexander T Toshev, Stephanie Wang, Dirk Groeneveld, Luca Soldaini, Pang Wei Koh, Jenia Jitsev, Thomas Kollar, Alex Dimakis, Yair Carmon, Achal Dave, Ludwig Schmidt, and Vaishaal Shankar. Datacomp-LM: In search of the next generation of training sets for language models. In *The Thirty-eight Conference on Neural Information Processing Systems Datasets and Benchmarks Track*, 2024. URL `https://openreview.net/forum?id=CNWdWn47IE`.

Zeming Lin, Halil Akin, Roshan Rao, Brian Hie, Zhongkai Zhu, Wenting Lu, Nikita Smetanin, Robert Verkuil, Ori Kabeli, Yaniv Shmueli, et al. Evolutionary-scale prediction of atomic-level protein structure with a language model. *Science*, 379(6637):1123–1130, 2023.

Zeyuan Liu, Zhihe Yang, Jiawei Xu, Rui Yang, Jiafei Lyu, Baoxiang Wang, Yunjian Xu, and Xiu Li. Adg: Ambient diffusion-guided dataset recovery for corruption-robust offline reinforcement learning. *arXiv preprint arXiv:2505.23871*, 2025.

Haoye Lu, Qifan Wu, and Yaoliang Yu. Stochastic forward–backward deconvolution: Training diffusion models with finite noisy datasets. In *Forty-second International Conference on Machine Learning*, 2025. URL https://openreview.net/forum?id=WrWqv3mpQx.

Gonzalo Martínez, Lauren Watson, Pedro Reviriego, José Alberto Hernández, Marc Juarez, and Rik Sarkar. Towards understanding the interplay of generative artificial intelligence and the internet. In *International Workshop on Epistemic Uncertainty in Artificial Intelligence*, pp. 59–73, 2023.

Chenlin Meng, Robin Rombach, Ruiqi Gao, Diederik Kingma, Stefano Ermon, Jonathan Ho, and Tim Salimans. On distillation of guided diffusion models. In *Proceedings of the IEEE/CVF conference on computer vision and pattern recognition*, pp. 14297–14306, 2023.

Nick Moran, Dan Schmidt, Yu Zhong, and Patrick Coady. Noisier2noise: Learning to denoise from unpaired noisy data. In *Proceedings of the IEEE/CVF conference on computer vision and pattern recognition*, pp. 12064–12072, 2020.

Bernt Oksendal. *Stochastic differential equations: an introduction with applications*. Springer Science & Business Media, 2013.

Vishakh Padmakumar and He He. Does writing with language models reduce content diversity? In *The Twelfth International Conference on Learning Representations*, 2024. URL https://openreview.net/forum?id=Feiz5HtCD0.

Mihir Prabhudesai, Mengning Wu, Amir Zadeh, Katerina Fragkiadaki, and Deepak Pathak. Diffusion beats autoregressive in data-constrained settings. *arXiv preprint arXiv:2507.15857*, 2025.

François Rozet, Gérôme Andry, Francois Lanusse, and Gilles Louppe. Learning diffusion priors from observations by expectation maximization. In *The Thirty-eighth Annual Conference on Neural Information Processing Systems*, 2024. URL https://openreview.net/forum?id=7v88Fh6iSM.

Chitwan Saharia, William Chan, Saurabh Saxena, Lala Li, Jay Whang, Emily L Denton, Kamyar Ghasemipour, Raphael Gontijo Lopes, Burcu Karagol Ayan, Tim Salimans, et al. Photorealistic text-to-image diffusion models with deep language understanding. *Advances in neural information processing systems*, 35:36479–36494, 2022.

Tim Salimans and Jonathan Ho. Progressive distillation for fast sampling of diffusion models. *arXiv preprint arXiv:2202.00512*, 2022.

Mohamed El Amine Seddik, Suei-Wen Chen, Soufiane Hayou, Pierre Youssef, and Merouane Abdelkader DEBBAH. How bad is training on synthetic data? a statistical analysis of language model collapse. In *First Conference on Language Modeling*, 2024. URL https://openreview.net/forum?id=t3z6UlV09o.

Vikash Sehwag, Xianghao Kong, Jingtao Li, Michael Spranger, and Lingjuan Lyu. Stretching each dollar: Diffusion training from scratch on a micro-budget. In *Proceedings of the Computer Vision and Pattern Recognition Conference*, pp. 28596–28608, 2025.

Kulin Shah, Alkis Kalavasis, Adam Klivans, and Giannis Daras. Does generation require memorization? creative diffusion models using ambient diffusion. In *Forty-second International Conference on Machine Learning*, 2025. URL https://openreview.net/forum?id=GGPM0z3dhU.

Piyush Sharma, Nan Ding, Sebastian Goodman, and Radu Soricut. Conceptual captions: A cleaned, hypernymed, image alt-text dataset for automatic image captioning. In Iryna Gurevych and Yusuke Miyao (eds.), *Proceedings of the 56th Annual Meeting of the Association for Computational Linguistics (Volume 1: Long Papers)*, pp. 2556–2565, Melbourne, Australia, July 2018. Association for Computational Linguistics. doi: 10.18653/v1/P18-1238. URL https://aclanthology.org/P18-1238/.

Ilia Shumailov, Zakhar Shumaylov, Yiren Zhao, Nicolas Papernot, Ross Anderson, and Yarin Gal. Ai models collapse when trained on recursively generated data. *Nature*, 631(8022):755–759, 2024.

Jascha Sohl-Dickstein, Eric Weiss, Niru Maheswaranathan, and Surya Ganguli. Deep unsupervised learning using nonequilibrium thermodynamics. In Francis Bach and David Blei (eds.), *Proceedings of the 32nd International Conference on Machine Learning*, volume 37 of *Proceedings of Machine Learning Research*, pp. 2256–2265, Lille, France, 07–09 Jul 2015. PMLR. URL `https://proceedings.mlr.press/v37/sohl-dickstein15.html`.

Gowthami Somepalli, Vasu Singla, Micah Goldblum, Jonas Geiping, and Tom Goldstein. Diffusion art or digital forgery? investigating data replication in diffusion models. In *Proceedings of the IEEE/CVF conference on computer vision and pattern recognition*, pp. 6048–6058, 2023a.

Gowthami Somepalli, Vasu Singla, Micah Goldblum, Jonas Geiping, and Tom Goldstein. Understanding and mitigating copying in diffusion models. In *Thirty-seventh Conference on Neural Information Processing Systems*, 2023b. URL `https://openreview.net/forum?id=HtMXRGbUMt`.

Yang Song and Stefano Ermon. Generative modeling by estimating gradients of the data distribution. In *Advances in Neural Information Processing Systems*, pp. 11895–11907, 2019.

Yang Song, Jascha Sohl-Dickstein, Diederik P Kingma, Abhishek Kumar, Stefano Ermon, and Ben Poole. Score-based generative modeling through stochastic differential equations. In *International Conference on Learning Representations*, 2021. URL `https://openreview.net/forum?id=PxTIG12RRHS`.

Yang Song, Prafulla Dhariwal, Mark Chen, and Ilya Sutskever. Consistency models. 2023.

Charles M Stein. Estimation of the mean of a multivariate normal distribution. *The annals of Statistics*, pp. 1135–1151, 1981.

Keqiang Sun, Junting Pan, Yuying Ge, Hao Li, Haodong Duan, Xiaoshi Wu, Renrui Zhang, Aojun Zhou, Zipeng Qin, Yi Wang, Jifeng Dai, Yu Qiao, Limin Wang, and Hongsheng Li. Journeydb: A benchmark for generative image understanding, 2023. URL `https://arxiv.org/abs/2307.00716`.

Ayush Tewari, Tianwei Yin, George Cazenavette, Semon Rezchikov, Josh Tenenbaum, Frédo Durand, Bill Freeman, and Vincent Sitzmann. Diffusion with forward models: Solving stochastic inverse problems without direct supervision. *Advances in Neural Information Processing Systems*, 36:12349–12362, 2023.

Maurice CK Tweedie. Statistical properties of inverse gaussian distributions. i. *The Annals of Mathematical Statistics*, 28(2):362–377, 1957.

Zijie J Wang, Evan Montoya, David Munechika, Haoyang Yang, Benjamin Hoover, and Duen Horng Chau. Diffusiondb: A large-scale prompt gallery dataset for text-to-image generative models. *arXiv preprint arXiv:2210.14896*, 2022.

Jinghui Zhang, Dandan Qiao, Mochen Yang, and Qiang Wei. Regurgitative training: The value of real data in training large language models. *arXiv preprint arXiv:2407.12835*, 2024.

Yasi Zhang, Tianyu Chen, Zhendong Wang, Ying Nian Wu, Mingyuan Zhou, and Oscar Leong. Restoration score distillation: From corrupted diffusion pretraining to one-step high-quality generation. *arXiv preprint arXiv:2505.13377*, 2025.

A Additional image results and ablations

A.1 Number of posterior samples

A natural ablation to consider is the multiplicity of posterior samplings performed during restoration. Concretely, while for all our experiments in the main paper we did posterior sampling exactly once for each corrupted sample, we can also choose to sample many times from the model using the same corrupted image. As this effectively multiplies the amount of corrupted data in our training set, we duplicate the clean data by the same amount to maintain balance. We see results for training on the multiplied datasets in Table 4 in the case of Blur ($\sigma_B = 0.6$) for the first loop. We observe that for the multiplicities considered (x1, x2, x4), more restorations improve FID.

Table 3: Comparison of restoration methods. FID ↓ (lower is better). Loop2 restorations.

Corruption		Restore from scratch	Restore from previous loop
Blur	$\sigma_B = 0.6$	3.862	**3.478**
	$\sigma_B = 0.8$	4.481	**4.156**
JPEG	$q = 25$	4.789	**4.318**
	$q = 18$	5.260	**4.678**

Table 4: Effect of number of posterior samples. Cifar Blur 0.6

Posterior samples	FID
x1	4.85
x2	4.70
x4	**4.52**

A.2 Choice of dataset to restore

In all our experiments in the main paper, we perform the restoration of each DataLoop always starting from the same corrupted samples. In this section, we ablate this choice by comparing to restoring from the previous DataLoop's restoration i.e. treating them as corrupted samples at a smaller noise level. Table 3 shows conditional FID of the restored dataset in Loop 2 if we restore from scratch vs continuing from the previous loop (Loop 1), in the case of Blur ($\sigma_B = 0.6$). We observe that restoring from the previous loop's dataset, to the effect of "trusting" the previous loop's model, actually leads to better conditional FID than restoring from scratch. This shows that errors can accumulate even as models get better from one loop to another.

A.3 Origin of improvement in terms of diffusion times

We also analyze where, in terms of noise times, the improved performance of the Ambient Loops model is coming from compared to the baseline Ambient Omni model. Figure 4 shows average EDM loss curves across different noise times averaged over the entire clean cifar-10 dataset, providing a window of analysis into the per-noise performance of the models. We observe that, for all four corruptions, the Loop1 models are better *for all noise times* than the Omni models. This is initially surprising as Ambient Loops can only facilitate the learning of information present in the dataset (the low-frequencies of the corrupted data), but can do nothing to recover information lost to the corruption (high-frequencies of the corrupted data). The conundrum is explained by the theoretical results: the posterior estimated samples are closer distributionally to the clean samples than the initial blurry samples, and so it is possible to extract more information from them at all noise levels. Indeed, the conditional FID results empirically support this assumption, as seen in 1: the corrupted datasets have conditional FIDs in the 10 to 60 range depending on the severity of the corruption, but the Loop 0 restored datasets all have FIDs below 5.

A.4 Posterior sampling noise schedule

Table 5 ablates the number of loops under different denoising schedulings for our looping algorithm.

Table 5: Ablation on Loop1 time-step and number of DataLoops for CIFAR10-32x32 under blur corruption ($\sigma_B = 0.6$). Metric: FID ↓.

	Ambient Omni (Loop 0)		Loop 1		Loop 2		Loop 3	
Loop1 time-step	Uncond. FID	Cond. FID	Uncond. FID	Cond. FID	Uncond. FID	Cond. FID	Uncond. FID	Cond. FID
0.20	5.34	3.92	5.20	3.86	4.76	**3.29**	4.67	4.15
0.10	5.34	3.92	4.69	3.81	4.92	3.32	-	-
0.05	5.34	3.92	**4.66**	3.86	4.77	3.47	-	-
0.00	5.34	3.92	4.77	3.88	-	-	-	-

B Proteins Appendix

B.1 Metrics

Backbone-only generative protein models are principally evaluated with two metrics: designability and diversity.

Designability measures the quality of generated proteins. 100 backbones each of lengths 50, 100, 150, 200, and 250 are generated by the model. To assess whether these backbones could actually be

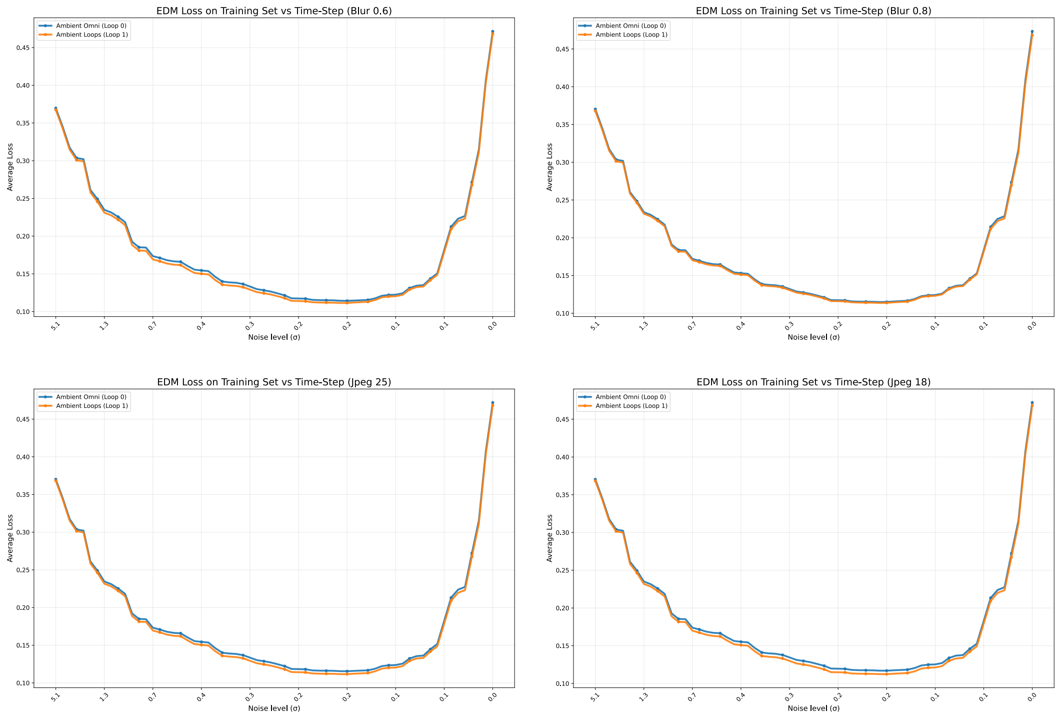

Figure 4: EDM loss vs noise level for Ambient Diffusion Omni Daras et al. (2025c) vs Ambient Loops (Loop 1) models across four corruptions on Cifar-10. Loops models have increased denoising performance *across all* noise levels for all four corruptions.

made by some sequence, ProteinMPNN Dauparas et al. (2022) is used to generate eight candidate amino acid sequences per backbone. These are then folded back into structures using ESMFold Lin et al. (2023), and if any of these is sufficiently close to the original backbone (RMSD < 2 Å), the backbone is considered designable. Designability is then defined as the percentage of generated backbones which are designable.

Diversity measures whether a set of generated structures is highly redundant or if it contains a wide array of meaningfully different proteins. To evaluate diversity, Foldseek is used to cluster the set of designable backbones with a TM-score threshold of 0.5. Diversity is defined as:

$$\text{Diversity} = \frac{\text{Number of Clusters}}{\text{Number of Designable Proteins}}$$

In practice, designability and diversity are at odds. Maximizing diversity typically requires generating less likely structures, some of which will not be designable.

B.2 Additional Results

Table 6: **Designability and diversity for protein structure generation.**

Model	**Designability (%↑)**	**Diversity (↑)**
Ambient Proteins (L0, $\gamma = 0.35$)	**99.2**	0.615
Ambient Loops (L1, $\gamma = 0.35$)	99.0	**0.703**
Proteina (FS $\gamma = 0.35$)	98.2	0.49
Genie2	95.2	0.59
FoldFlow (base)	96.6	0.20
FoldFlow (stoc.)	97.0	0.25
FoldFlow (OT)	97.2	0.37
FrameFlow	88.6	0.53
RFDiffusion	94.4	0.46
Proteus	94.2	0.22

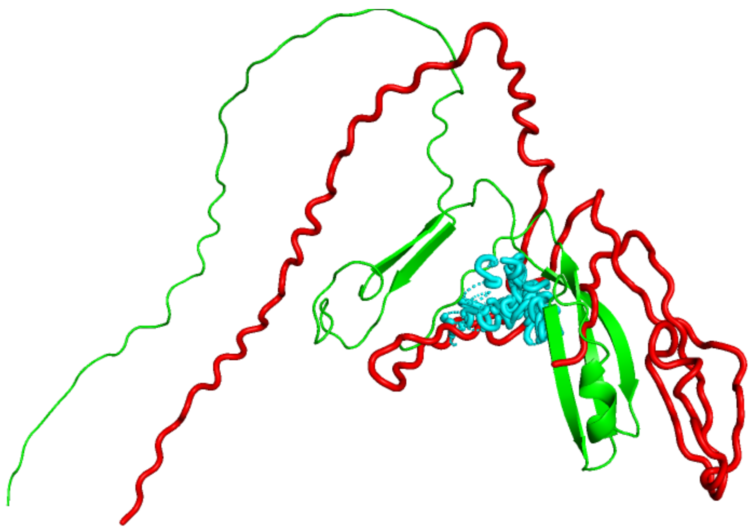

Figure 5: Example denoising (red) of a noisy version (cyan) of the green protein.

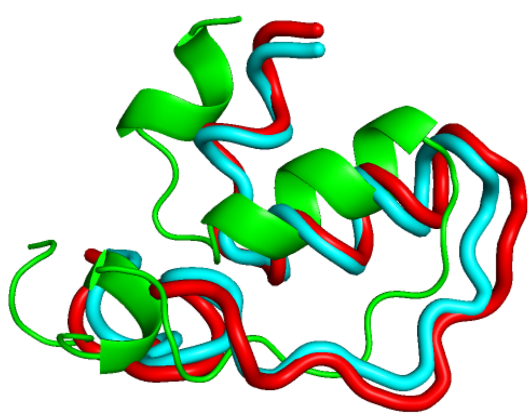

Figure 6: Example denoising (red) of a noisy version (cyan) of the green protein.

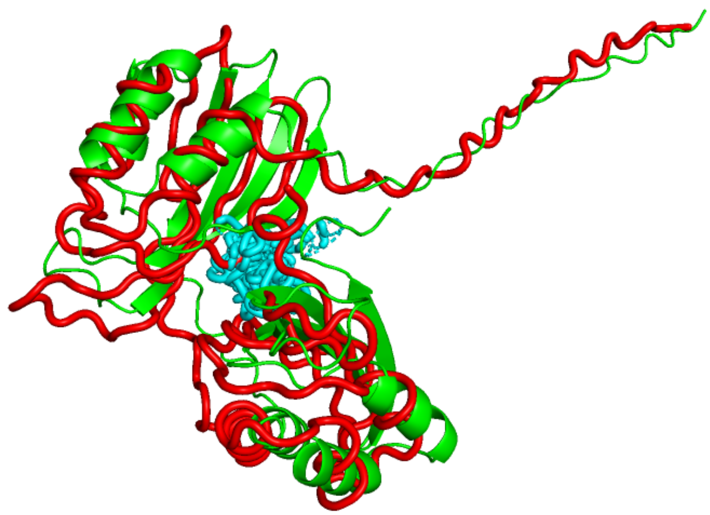

Figure 7: Example denoising (red) of a noisy version (cyan) of the green protein.

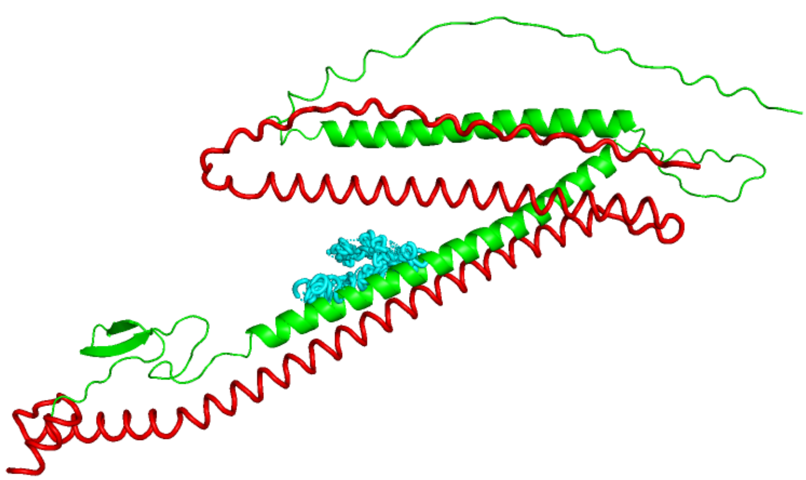

Figure 8: Example denoising (red) of a noisy version (cyan) of the green protein.